

Article

Estimation and Comparison of SOC in Batteries Used in Electromobility Using the Thevenin Model and Coulomb Ampere Counting

Diego Salazar * and Marcelo Garcia 

Research Group on Smart Electrical Networks (GIREI), South Campus, Quito Headquarters,
School of Engineering, Universidad Politecnica Salesiana, Cuenca 010105, Ecuador

* Correspondence: steven_salazar23@hotmail.com

Abstract: Nowadays, due to the increasing use of electric vehicles, manufacturers are making more and more innovations in the batteries used in electromobility, in order to make these vehicles more efficient and provide them with greater autonomy. This has led to the need to evaluate and compare the efficiency of different batteries used in electric vehicles to determine which one is the best to be implemented. This paper characterises, models and compares three batteries used in electromobility: lithium-ion, lead-acid, and nickel metal hydride, and determines which of these three is the most efficient based on their state of charge. The main drawback to determine the state of charge is that there are a great variety of methods and models used for this purpose; in this article, the Thévenin model and the Coulomb Count method are used to determine the state of charge of the battery. When obtaining the electrical parameters, the simulation of the same is carried out, which indicates that the most efficient battery is the Lithium-ion battery presenting the best performance of state of charge, reaching 99.05% in the charging scenario, while, in the discharge scenario, it reaches a minimum value of 40.68%; in contrast, the least efficient battery is the lead acid battery, presenting in the charging scenario a maximum value of 98.42%, and in the discharge scenario a minimum value of 10.35%, presenting a deep discharge. This indicates that the lithium-ion battery is the most efficient in both the charge and discharge scenarios, and is the best option for use in electric vehicles. In this paper, it was decided to use the Coulomb ampere counting method together with the Thévenin equivalent circuit model because it was determined that the combination of these two methods to estimate the SOC can be applied to any battery, not only applicable to electric vehicle batteries, but to battery banks, BESS systems, or any system or equipment that has batteries for its operation, while the models based on Kalman, or models based on fuzzy mathematics and neural networks, as they are often used and are applicable only to a specific battery system.



Citation: Salazar, D.; Garcia, M. Estimation and Comparison of SOC in Batteries Used in Electromobility Using the Thevenin Model and Coulomb Ampere Counting. *Energies* **2022**, *15*, 7204. <https://doi.org/10.3390/en15197204>

Academic Editors: Danial Karimi and Amin Hajizadeh

Received: 2 August 2022

Accepted: 24 August 2022

Published: 30 September 2022

Publisher's Note: MDPI stays neutral with regard to jurisdictional claims in published maps and institutional affiliations.



Copyright: © 2022 by the authors. Licensee MDPI, Basel, Switzerland. This article is an open access article distributed under the terms and conditions of the Creative Commons Attribution (CC BY) license (<https://creativecommons.org/licenses/by/4.0/>).

Keywords: electric batteries; state of charge; electromobility; nickel metal hydride; lithium-ion; lead acid

1. Introduction

Currently, the growing use of electric vehicles has become a powerful alternative to combustion vehicles, due to concerns about environmental damage and climate change caused by greenhouse gases; electric vehicles are presented as the alternative to combustion vehicles, which seeks to reduce or eliminate the pollution caused by combustion vehicles [1].

In 1910, electric vehicles (EVs) could be seen on the streets and avenues, but they were quickly replaced by combustion vehicles because EVs had low efficiency, high costs, and low speed compared to their combustion vehicle counterparts. An EV harnesses electrical energy stored in one or more batteries to produce motion, using a motor. The high demand for EVs presents electric vehicle manufacturers and developers with major challenges in developing more efficient vehicles with greater range. In the last decade, battery technology

used in EVs has improved enormously, increasing efficiency and battery life, which has always been the weakest point of EVs [1,2].

To meet the goal of future transport with more efficient vehicles and with low or zero emissions of greenhouse gases emitted by current vehicles, electric vehicles (EV), hybrid electric vehicles (HEV), and plug-in hybrid vehicles (PHEV) are emerging as the best alternative currently available to reduce the pollution caused by a conventional vehicle [3].

The electric battery is the most important component in the electric vehicle as it supplies and stores energy for the electric vehicle to operate, has the greatest impact on efficiency and range, is also the heaviest component of the EV, and must be strategically placed within the vehicle to provide stability through a low centre of gravity [4,5].

Due to the importance and impact that the battery has on the efficiency and operation of the EV, models have been created to estimate and know the energy stored inside the battery and, in this way, to predict the behaviour in different charging and discharging events; and to carry out an efficient management of the energy stored in the battery [6].

For battery energy management, the State of Charge (SOC) is estimated, which indicates the remaining energy in the battery, and the battery performance is determined on the basis of the SOC [6,7].

EVs use electric batteries to supply power to the synchronous motor and thus produce motion in the vehicle. Currently, the number of electric vehicles has increased rapidly due to their greater efficiency and range. With technological development driven by the high demand for EVs, EV manufacturers are finding better and better production methods and materials to increase battery life and reduce charging times. EVs use electric batteries to supply power to the synchronous motor and thus produce motion in the vehicle. Today, the number of electric vehicles has increased rapidly due to their increased efficiency and range. With technological development driven by the high demand for EVs, EV manufacturers are increasingly finding better production methods and materials to increase battery life and reduce charging times [8].

Within electric vehicles, there are HEVs (hybrid electric vehicles), which use a combustion engine, one or more electric batteries and an electric motor for their operation. These vehicles are considered as a solution to reduce pollutant gas emissions in the short and medium term [9].

Another variation of an EV is the PHEV (plug-in hybrid electric vehicle), which is presented as progress towards 100% emission-free vehicles, the PHEV includes the best features of an EV and can also charge its batteries using grid outlets or a diesel generator, which enhances the advantages of a current HEV [10].

Several models have been developed to estimate the state of charge, such as the one proposed in [11], present an estimation of SOC by obtaining the open circuit voltage or internal voltage (V_{oc}) of the battery using the Thévenin equivalent model; in this research, the relationship between the V_{oc} and the state of charge is taken into account, which allows by using the Recursive-Least-Square algorithm, to estimate the state of charge and the internal parameter of the battery, with a very low estimation error.

In [12], SOC estimation is carried out to determine the behaviour of the internal temperature present in the battery. To make this estimation, the researchers took into account the electrochemical model of the lithium-ion battery; their research determined a linear relationship between the charge and discharge of the battery at different current values, and the behaviour of the temperature, presenting higher temperatures at the time of discharge.

In [13], the Coulomb Count method and fuzzy mathematics were used to perform the estimation, together with the CCM method; this state of charge estimation was performed experimentally on a Lithium-ion battery, in order to identify the behaviour of the state of charge under different scenarios of charge and discharge of the battery; this research also presents a low error of state of charge estimation which indicates that this method is efficient and reliable when performing this estimation and determining the internal parameters of the battery.

For the above mentioned, in order to prolong the lifetime of electric batteries used in electromobility, a management system must be developed, allowing the user to better manage the operation and wear of the battery, increasing safety, reliability and efficiency [14].

The Coulomb ampere-counting model is a model that is easy to implement for SOC estimation, and the estimation pressure may depend on the operating and simulation conditions, which is why it was decided to use this method together with the Thévenin model to estimate the SOC of batteries used in electromobility [15], in order to compare the performance of each battery and thus determine which is the best battery to be implemented in electro mobility.

By carefully studying the papers cited above, it can be seen that there is a wide variety of methods and models used in order to estimate the state of charge of the battery, but there is a drawback in each of the models mentioned above; this drawback lies in the fact that these models can only be used for a specific type of battery, that is, they cannot be applied to all existing batteries used in electromobility without sacrificing their efficiency and low error rate. It is for this reason that the present research article seeks to find and estimate the state of charge using a unique and universal model, through the Coulomb ampere count and the Thévenin model, to be implemented in all existing electric batteries, without sacrificing efficiency and maintaining a low error rate.

2. Electric Batteries

EVs use electric batteries to supply power to the engine to propel the vehicle. The success of EVs depends on the energy stored in the batteries to provide the low-cost, reliable and safe performance and range required for use in an EV [16].

The most used electric batteries in electromobility are [5].

- Lithium-ion;
- Nickel metal hydride (NIMH);
- Lead Acid.

Lithium-ion batteries are currently the best choice for storing energy for an EV, as they feature: long cycle life to increase battery life, high energy density, no memory effect and a low self-discharge rate [3]. These advantages have made this type of batteries so popular and used nowadays, especially in the field of electro mobility; however, the most negative point of this type of batteries is that they need protection during their charge and discharge cycles [3,17,18].

Ni-MH batteries have emerged as one of the most promising solutions, as they have excellent advantages such as: excellent power-to-weight ratio, fast charging, environmentally friendly manufacturing, low self-discharge rate and no memory effect [19,20]. Thanks to these features present in the Ni-MH battery, these batteries are receiving more attention from electric vehicle manufacturers [21,22].

Lead-acid batteries are in high demand by EV manufacturers, due to their excellent features such as: low cost, high energy density, high energy storage capacity, low energy consumption and high energy efficiency [20,23]. This type of batteries is the most abundant as their components are widely available and their recyclability is high [20,24].

3. Methodology and Characterization of Batteries

The paper considers Lithium-Ion, Lead Acid and Nickel Metal Hydride batteries for characterisation, modelling and comparison, using Thévenin's equivalent circuit model and Coulomb Ampere counting to model and simulate the proposed electric batteries. Simulation of the electrical parameters of the battery will also be carried out to estimate the SOC and the charge and discharge time in the batteries [21,25].

SOC estimation is a challenge for all researchers seeking to determine the efficiency of batteries, as a correct estimation of SOC will increase the lifetime of the battery because it allows us to properly manage the energy stored in the battery and will protect it against overcharge or deep discharge [6]. The most common expression for estimating the SOC of a battery is given in Equation (1) [25,26]:

$$SOC(t) = SOC(t_0) - \frac{n_c}{C} \int_0^t i(t) dt \quad (1)$$

where

$SOC(t_0)$ is the initial value of the SOC at time 0; n_c is the efficiency of the battery $i(t)$ in the instantaneous value of the charging or discharging current C at rated battery capacity.

The Coulomb counting method together with the Thévenin model is widely used to estimate the SOC, thanks to its easy application to all types of batteries, since it considers the nominal capacity and the current of the battery under charge or discharge as shown in Figure 1 [27].

In order to use this method, the initial SOC, the voltage and the charge or discharge current of the batteries must be known, and it must be complemented with a proportional regulator, since the estimation error increases with time [27].

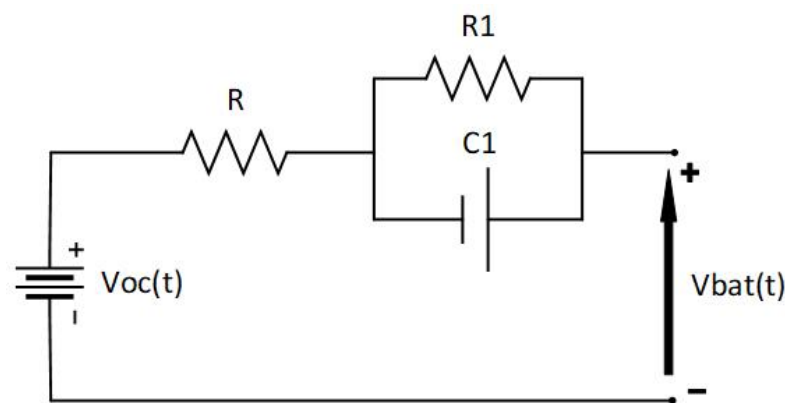


Figure 1. Thevenin equivalent model used for state of charge estimation in electric batteries, where R is the internal resistance of the battery, $R1$ is the resistance of the electrochemical present in the battery and $C1$ is the capacitance of the battery.

In [28], SOC estimation by Coulomb Counting is used in conjunction with the Thévenin model, taking into account the battery terminal voltage and the initial SOC.

Ref. [28] indicates that, in order to have a more accurate estimate, a modification to the traditional Thévenin model should be made, making it bidirectional to improve the estimation pressure.

Figure 2 shows a simplified bidirectional model for a more accurate estimation, dependent on the direction of the current; this model distinguishes whether the current is positive or negative, i.e., whether the battery is discharging or charging, to obtain the SOC for both scenarios [29].

Another variant of the Thévenin model is shown in Figure 2, and is used for SOC estimation, where the battery is considered as an ideal voltage source and a series resistor [29], where it can be determined that

$$V_{bat}(t) = V_{oc}(t) + R_{int} * i(t) dt \quad (2)$$

In [29], an estimation of SOC using the Coulomb counter and the Thévenin model is proposed; to perform this estimation, the $V_{oc}(t)$ (Battery Internal Voltage) is added in the model:

$$SOC(t) = SOC(t_0) + \frac{1}{SOC_m} \int_0^t \frac{i(t)}{3600} dt \quad (3)$$

where SOC_0 is the initial charge state. SOC_m is the maximum battery power; $i(t)$ is the charging or discharging current battery; and $V_{oc}(t)$ is the internal battery voltage $SOC(t)$ is the state of charge.

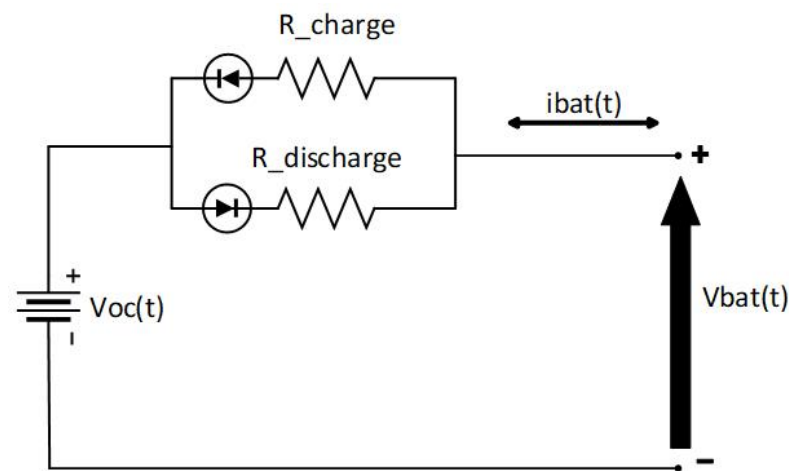


Figure 2. Equivalent simplified Thevenin model, used for precise estimation of the SOC.

To calculate V_{co} , a linear relationship is established with the SOC, where V_{co} at discharge is represented in Equation (4):

$$V_{oc}(t) = ns * (2 + 0.148 * B) \quad (4)$$

$$B = \frac{SOC(t)}{SOCm} \quad (5)$$

where

ns is the number of cells in the battery.

Internal Battery Voltage (V_{co}) on Charge

$$V_{oc}(t) = ns * (1.926 + 0.124 * B) \quad (6)$$

In this model, the internal resistance is assumed to be constant; with this parameter, the battery voltage is calculated. Assuming a constant value for the internal resistance of the battery causes the estimation error to be quite considerable [29].

To correct this error of constant values in the battery components, in the [30], a modification is proposed, to estimate the internal elements of the battery as a function of the SOC; the proposed modification is shown in Figure 3.

In order to estimate the state of charge, a modification is made to the model presented in [29]; this modification, as shown in Figure 3, allows for estimating each electrical parameter of the battery depending on the state of charge.

In [30], it is proposed to calculate the battery terminal voltage by characterising V_{co} , R_1 , R_2 , and C_1 , which have a linear relationship with the SOC. The internal resistance of the battery can be calculated by knowing the values of $V_{oc}(t)$, $V_{bat}(t)$ and $I_{bat}(t)$. The resistance (R) must be calculated for the charge and discharge scenario, as shown in Equation (7):

$$R = \frac{V_{oc}(t) - V_{bat}(t)}{I_{bat}(t)} \quad (7)$$

It is important to determine a correction factor β for the estimation of the internal resistance of the battery during charging and discharging. β is dependent on SOC and current. It is important to overcome the factor β by two, one for discharge and one for load, to avoid estimation errors [7].

The factor β is obtained by the ratio between the instantaneous resistance (R_i), the instantaneous resistance is obtained by Equation (7) and the load resistance (R_c) or discharge resistance (R_d):

$$B = \frac{R_i}{R_c} \quad (8)$$

$$B = \frac{R_i}{R_d} \quad (9)$$

Knowing the value of the correction factor β , it is possible to perform the linear relationship between the current, the SOC and the resistance; to determine the β value, Equation (9) is used [7]:

$$BC = -0.72947 * I_{bat}(t) + 0.81 \quad (10)$$

$$Bd = 1.0221 * I_{bat}(t) + 1.1087 \quad (11)$$

where

B_c is the correction factor for charge.

B_d is the correction factor for discharge.

It was decided to limit β to a maximum value of 0.94 [31] for lithium-ion battery, 0.8 [31] for the Lead Acid battery, and of 0.89 [32] for the Nickel Metal Hydride battery.

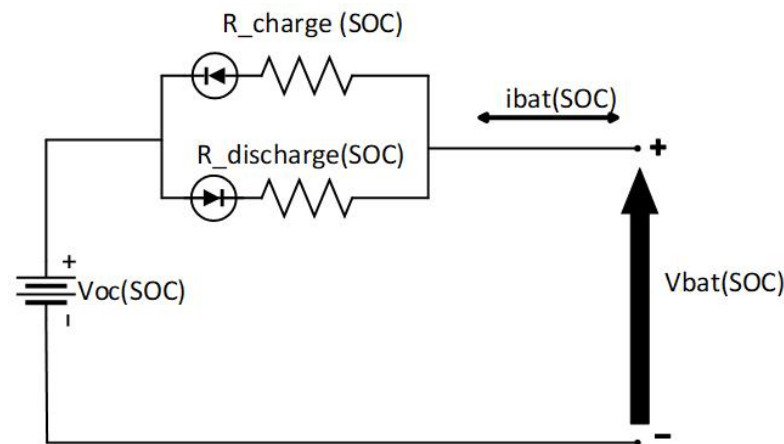


Figure 3. Thevenin equivalent model proposed in [29], where the electrical parameters are calculated as a function of the SOC.

To correct the error present in the Ampere Counting method, a proportional regulator is calculated to reduce the error to a minimum.

The proportional regulator is calculated using the error (e) of the comparison of the voltage at the battery terminals and the estimated voltage of the battery; this error is multiplied by a constant K_p , resulting in the variation of SOC (ΔSOC) [7].

$$\Delta SOC = R_p * e \quad (12)$$

The disadvantage of Equation (12) is that, to determine the value of K_p , the error is unknown, which varies over time and is obtained by simulating the electric batteries [7]. Therefore, first the simulation is carried out, without the proportional regular and obtain the average error of each battery, data are obtained that the average error is 0.28 [V], for the Lithium-Ion battery, 0.23 [V] for the Lead Acid battery and 0.13 [V] for the Nickel Metal Hydride battery.

Noting that the SOC of each battery varies by approximately 20% every hour, we can find the value of K_p [7]

$$\Delta SOC = \frac{\Delta SOC}{s} = \frac{20\%}{3600[s]} = 5.56 \times 10^{-5} \quad (13)$$

$$\Delta SOC = \frac{\Delta SOC}{\frac{s}{\frac{e}{\frac{\Delta}{\Delta}}}} \quad (14)$$

Using Equation (14), the proportional regulator value for the lithium-ion battery is obtained to be

$$1.9857 \times 10^4 \quad (15)$$

for Lead Acid Battery

$$2.4174 \times 10^4 \quad (16)$$

and, for the nickel metal hydride battery, it is

$$4.2769 \times 10^4 \quad (17)$$

4. Results

In the present article, three batteries of 100 [Ah], Lithium-Ion, Lead-Acid, and Nickel Metal Hydride batteries, used in electro mobility, were taken. The metal hydride battery has a voltage of 12.5 [V], the lithium-ion battery has a voltage of 12.8 [V], and the lead acid battery has a voltage of 12 [V].

4.1. Discharge

Two scenarios were performed for the simulation (charging and discharging), for the discharging scenario, a random discharge current is used; the same current value is applied to the batteries proposed for this article; and the batteries are discharged to 64% (ideal battery) of the SOC, in a time of 6 h.

The data presented in Figure 4 show that the lithium-ion battery is the most efficient battery, with a better performance in its SOC compared to the metal hydride battery, reaching a performance of 40% SOC, the nickel battery represents an intermediate performance in its state of charge, discharging up to 24% SOC, while the metal hydride battery presents a 24.3% SOC; it is also observed that the lead acid battery is the least efficient battery, as it presents a deep discharge.

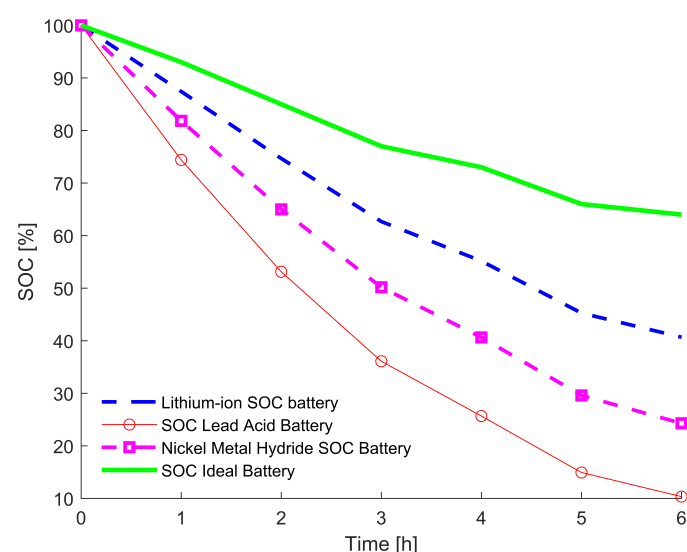


Figure 4. Comparison of the SOC curves, obtained in the discharge scenario.

Figure 5 shows the dynamic behaviour of the internal resistance of the battery, showing that the resistance value changes as a function of the SOC, indicating that, the greater

the discharge, the greater the power losses in the battery. In Figure 5, the resistance of the lithium-ion battery stands out as it presents high values with respect to the batteries, increasing significantly when the SOC reaches 90%, indicating that the losses in the discharge scenario are considerable, but, in spite of this, the lithium battery is the most efficient. For the resistances in the Lead Acid and Nickel Metal Hydride batteries, presenting lower values than those observed in the Lithium Ion battery, the figure also shows that, from 35% and 50% SOC, respectively, the resistance in the batteries starts to increase, indicating that, as the battery discharges, the losses increase and the SOC decreases.

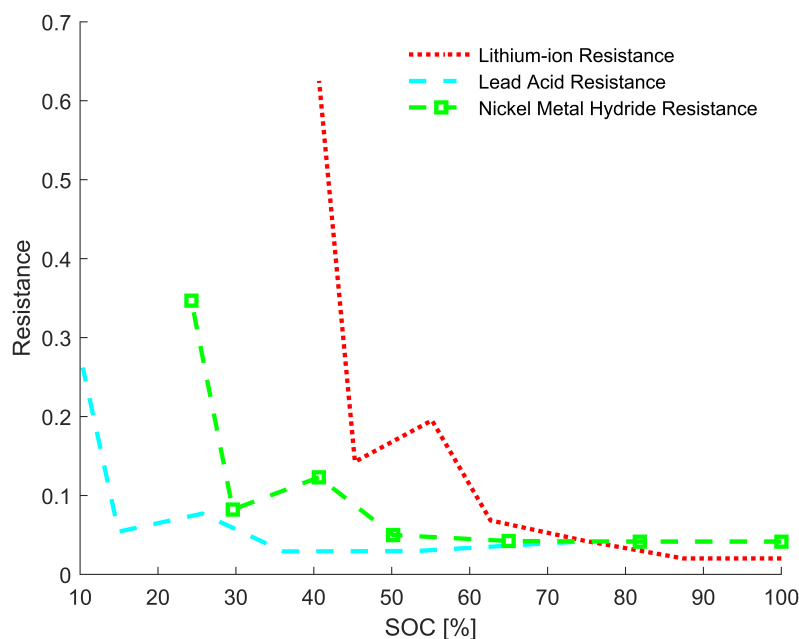


Figure 5. Comparison between the results obtained from the internal discharge resistance of the batteries studied in the article.

In Figure 6, the voltages obtained in the simulation are observed, the initial voltage in the lithium-ion battery is 12.8 volts when the SOC is at 100%, discharging an average of 0.3 [V], in each hour, reaching a value of 11.1 [V] at 40% of the SOC; in the case of the estimated voltage of the battery, it is observed that the values are very close to the values of the battery voltage, presenting a voltage of 12.81 [V], when the battery is 100% charged, a voltage of 11.47 [V], when reaching 40% of the SOC. In the Lead Acid battery, the initial voltage is 12 [V], reaching a value of 10.8 [V], discharging an average of 0.3 [V] every hour, the estimated voltage for this battery at 100% SOC is 12.5 [V], and 11.10 [V], when reaching 10% SOC. For the Nickel Metal Hydride battery, the battery voltage is 12.5 [V], reaching a minimum value of 11.6 [V]; in this battery, the estimated voltage at 100% SOC is 12.53 [V], while, at 20% state of charge, it is 11.80 [V].

The internal voltages in the lithium-ion battery are 13 [V], discharging linearly to 12.5 [V]; for the lead-acid battery, it is 12.3 [V], reaching a minimum value of 11.3 [V], and, for the nickel metal hydride battery, it is 12.8 [V], reaching a minimum value of 12.34 [V].

Figure 7 shows that the error obtained in the SOC estimation is very low, indicating that the method and models used are accurate and highly reliable for SOC estimation.

To calculate the SOC estimation error, the battery voltage and the estimated battery voltage were taken into account, and a comparison was made between both voltages, and the estimation error was determined, observing that the error gradually increases as the simulation progresses but does not exceed 5%, which indicates that the SOC estimation using the Thevenin model, and the amperage count is correct.

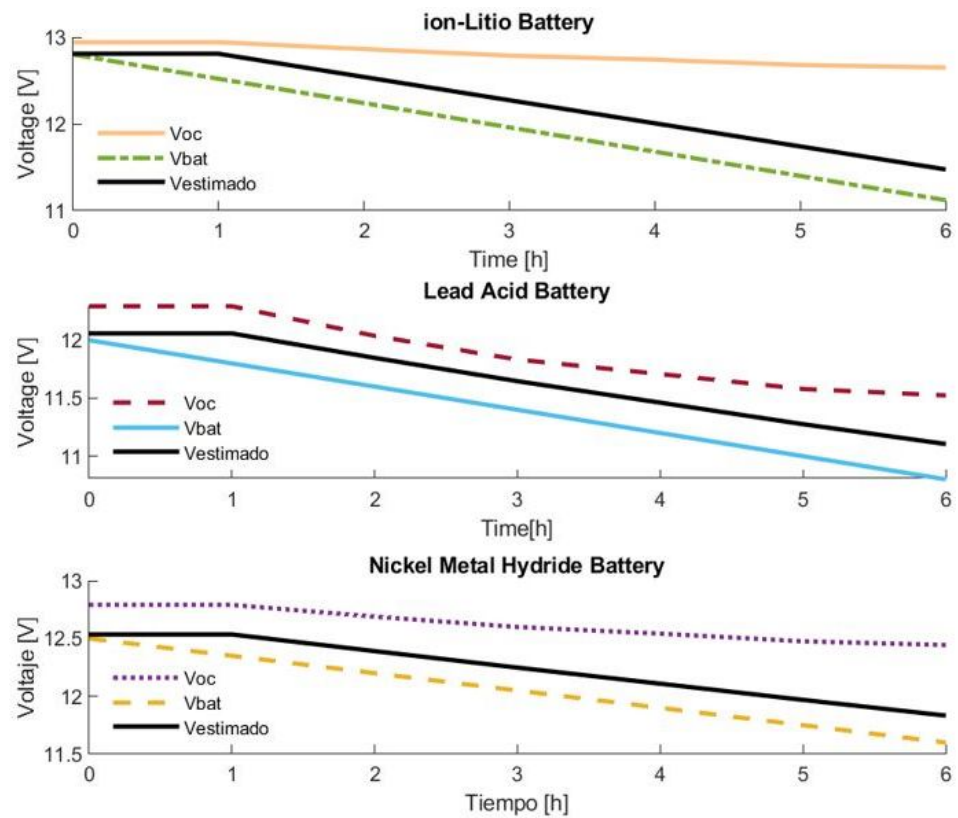


Figure 6. Discharge voltage at the terminals and estimated internal voltages of the electric batteries studied in the article.

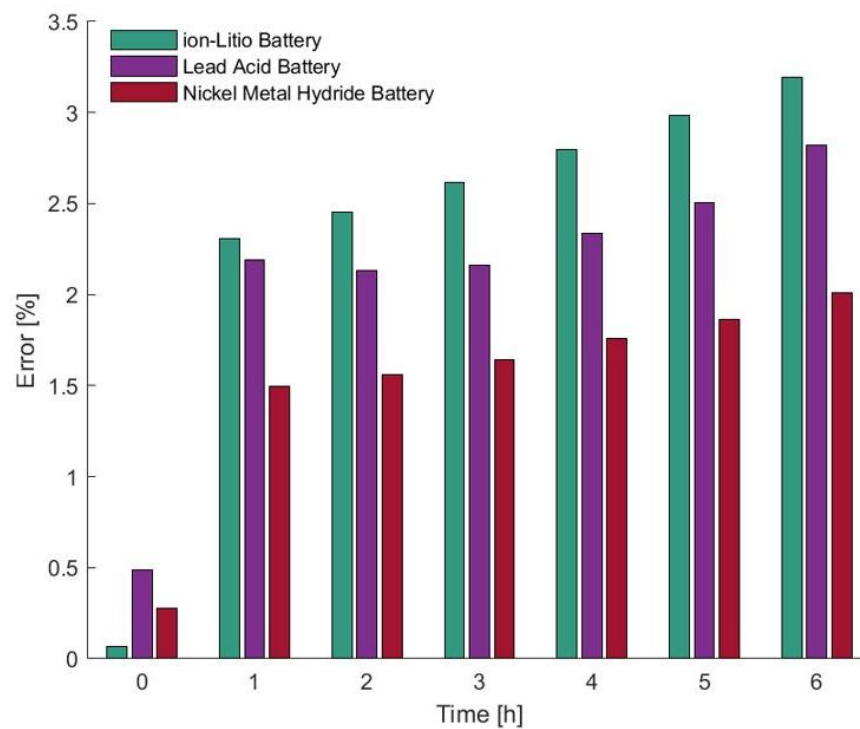


Figure 7. Errors obtained in the estimation of the SOC in the batteries studied in the article, in the discharge scenario.

4.2. Charge

In the charging scenario, a constant current of 12.5 [A], for a period of 5 h, is used to charge the battery; the initial SOC for this scenario is taken from the estimated SOC result of the discharge scenario, until a value close to 100% of the SOC is reached.

Figure 8 shows that the SOC starts from the final SOC value obtained in the discharge simulation. In this scenario, the lithium-ion battery again shows a higher efficiency at the time of charging compared to the lead-acid and nickel metal hydride batteries.

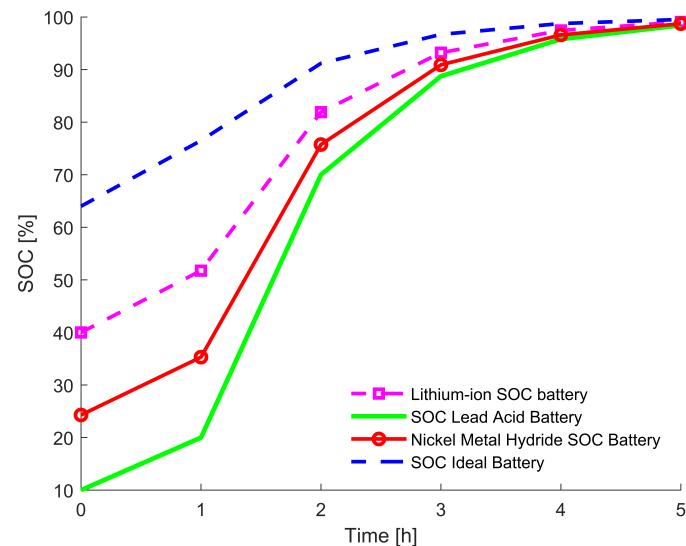


Figure 8. Comparison of the SOC curves, obtained in the charge scenario.

Figure 9 shows that the resistance increases from the moment the battery is charged, the resistance of the lithium-ion battery and the resistance of the metal hydride battery have similar values at SOC greater than 70%. This increase in the resistance of the batteries is due to the fact that the battery is closer to being charged, and indicates that the charge losses increase, which means that the battery must be charged for much longer in order to reach 100% charge. The resistance of the lead-acid battery is lower than that of the metal ion-lithium hydride battery, but despite having a lower resistance, it is the least efficient battery in the charging scenario.

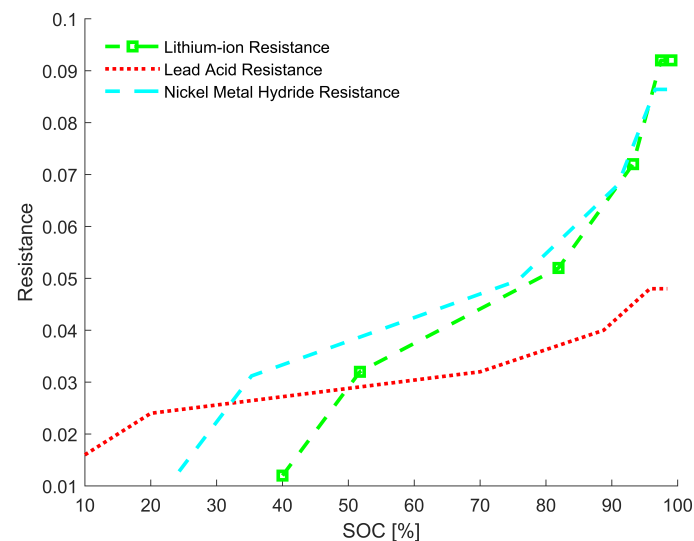


Figure 9. Comparison between the results obtained from the internal charge resistance of the batteries studied in the article.

Figure 10 shows that both the internal battery voltages and the terminal voltages are linearly charged, reaching their pre-discharge values.

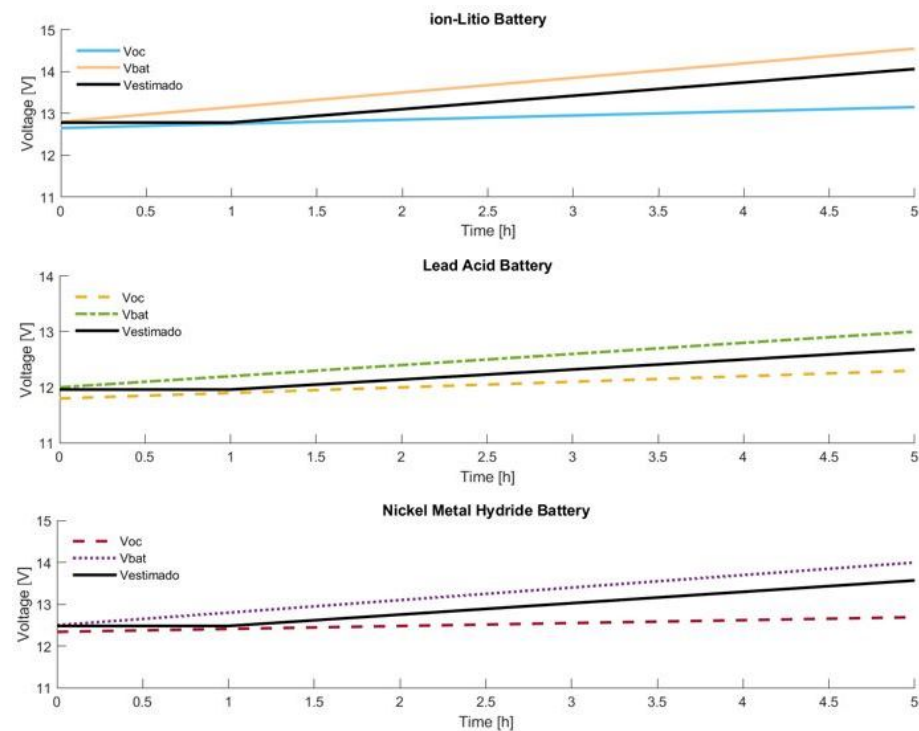


Figure 10. Charge voltage at the terminals and estimated internal voltages of the electric batteries studied in the article.

Figure 11 shows the error obtained in the simulation of the battery charging scenario, it can be seen that the error does not exceed 5% in any of the simulated batteries, which clearly indicates that this model is very accurate in estimating the SOC, and the battery voltages.

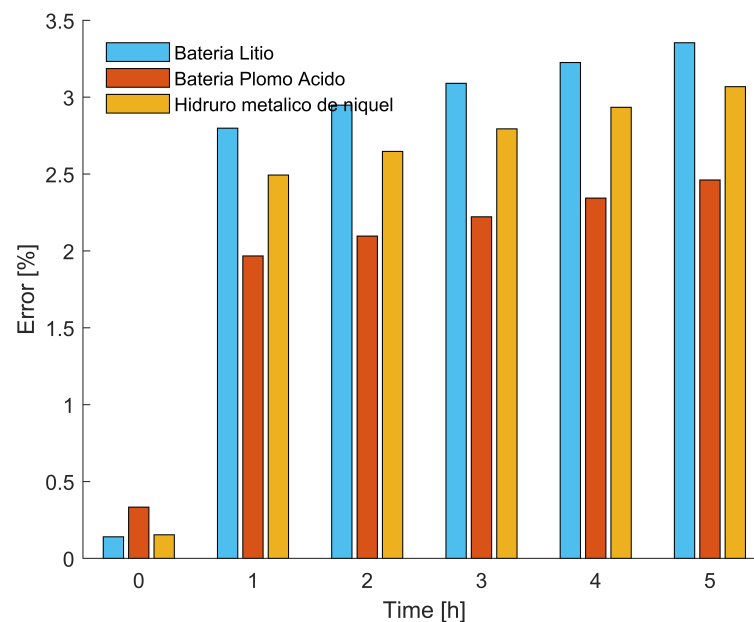


Figure 11. Errors obtained in the estimation of the SOC in the batteries studied in the article, in the charge scenario.

For the calculation of the estimation error, the battery voltage and the estimated voltage were taken into account, which is allowed by comparing both the estimation of the error. Observing that, as in the discharge scenario, the error increases as the simulation progresses, but without exceeding the maximum established range, indicating once again that the Thevenin model and ampere count is a recommendable option for estimating the SOC in the charge and discharge scenario, as it presents very low error values.

5. Conclusions

When analysing the data obtained in the simulation, it was determined that the battery with the best SOS performance is the Lithium-ion battery, both in the charge and discharge scenarios, reaching 99% and 40%, respectively, while the Lead Acid battery is the least efficient, reaching 10% of the SOC in the discharge scenario, presenting a deep discharge, and in the charge scenario reaching 98% of the SOC, when subjected to the same simulation conditions.

A correct estimation allows for making decisions and energy management strategies in batteries, to expand their useful life and improve their performance; however, at present, there is no effective method or model of estimation, and simple to implement, to estimate the SOC; for this reason, we must continue researching better and more complete methods to perform this task efficiently and with increasingly lower errors.

Author Contributions: Conceptualization, M.G.; Investigation, D.S. and M.G.; Supervision, M.G. All authors have read and agreed to the published version of the manuscript.

Funding: This research received no external funding.

Data Availability Statement: Not applicable.

Conflicts of Interest: The authors declare no conflict of interest.

References

1. Sreedhar, V. Plug-In Hybrid Electric Vehicles with Full Performance. In Proceedings of the 2006 IEEE Conference on Electric and Hybrid Vehicles, Pune, India, 18–20 December 2006.
2. Ruddle, A.R.; Galarza, A.; Sedano, B.; Unanue, I.; Ibarra, I.; Low, I.L. Safety and failure analysis of electrical powertrain for fully electric vehicles and the development of a prognostic health monitoring system. In Proceedings of the IET Hybrid and Electric Vehicles Conference 2013 (HEVC 2013), London, UK, 6–7 November 2013; pp. 1–6. [\[CrossRef\]](#)
3. Jiang, B.; Liu, Y.; Huang, X.; Prakash, R.R.R. A New Battery Active Balancing Method with Supercapacitor Considering Regeneration Process. In Proceedings of the IECON 2020 46th Annual Conference of the IEEE Industrial Electronics Society, Singapore, 18–21 October 2020; pp. 2364–2369. [\[CrossRef\]](#)
4. Brandl, M.; Gall, H.; Wenger, M.; Lorentz, V.; Giegerich, M.; Baronti, F.; Fantechi, G.; Fanucci, L.; Roncella, R.; Saletti, R.; et al. Batteries and battery management systems for electric vehicles. In Proceedings of the 2012 Design, Automation & Test in Europe Conference & Exhibition (DATE), Dresden, Germany, 12–16 March 2012; pp. 971–976. [\[CrossRef\]](#)
5. Ranawat, D.; Prasad, M.P.R. A Review on Electric Vehicles with perspective of Battery Management System. In Proceedings of the 2018 International Conference on Electrical, Electronics, Communication, Computer, and Optimization Techniques (ICEECCOT), Mysuru, India, 14–15 December 2018; pp. 1539–1544. [\[CrossRef\]](#)
6. Wahyuddin, M.I.; Priambodo, P.S.; Sudibyo, H. State of Charge (SoC) Analysis and Modeling Battery Discharging Parameters. In Proceedings of the 2018 4th International Conference on Science and Technology (ICST), Yogyakarta, Indonesia, 7–8 August 2018; pp. 2–6. [\[CrossRef\]](#)
7. Zabaleta, J.; San Martín, I.; Pascual, J. *Cálculo del Estado de Carga en Baterías de Plomo-ácido: Diseño y Validación Experimental*; Universidad Pública de Navarra: Navarra, Spain, 2016; p. 71.
8. Kiselev, A.; Kuznietsov, A. Motor drive control of a full-electric vehicle using generalized predictive control algorithm. In Proceedings of the 2014 IEEE International Electric Vehicle Conference (IEVC), Florence, Italy, 17–19 December 2014. [\[CrossRef\]](#)
9. Saleki, A.; Rezaade, S.; Changizian, M. Analysis and simulation of hybrid electric vehicles for sedan vehicle. In Proceedings of the 2017 Iranian Conference on Electrical Engineering (ICEE), Tehran, Iran, 2–4 May 2017; pp. 1412–1416. [\[CrossRef\]](#)
10. Sabri, M.M.; Danapalasingam, K.; Rahmat, M. A review on hybrid electric vehicles architecture and energy management strategies. *Renew. Sustain. Energy Rev.* **2016**, *53*, 1433–1442. [\[CrossRef\]](#)
11. Susanna, S.; Dewangga, B.R.; Wahyungoro, O.; Cahyadi, A.I. Comparison of simple battery model and thevenin battery model for SOC estimation based on OCV method. In Proceedings of the 2019 International Conference on Information and Communications Technology (ICOIACT), Yogyakarta, Indonesia, 24–25 July 2019; pp. 738–743. [\[CrossRef\]](#)
12. Zhu, J.; Sun, Z.; Wei, X.; Dai, H. A new lithium-ion battery internal temperature on-line estimate method based on electrochemical impedance spectroscopy measurement. *J. Power Sources* **2015**, *274*, 990–1004. [\[CrossRef\]](#)

13. Saji, D.; Babu, P.S.; Ilango, K. SoC Estimation of Lithium Ion Battery Using Combined Coulomb Counting and Fuzzy Logic Method. In Proceedings of the 2019 4th International Conference on Recent Trends on Electronics, Information, Communication & Technology (RTEICT), Bangalore, India, 17–18 May 2019; pp. 948–952. [\[CrossRef\]](#)
14. Yu, D.X.; Gao, Y.X. SOC estimation of lithium-ion battery based on Kalman filter algorithm. *Appl. Mech. Mater.* **2013**, *347–350*, 1852–1855. [\[CrossRef\]](#)
15. Gissero, A.; Schaltz, E.; Stroe, D.-I. Recursive State of Charge and State of Health Estimation Method for Lithium-Ion Batteries Based on Coulomb Counting and Open Circuit Voltage. *Energies* **2020**, *13*, 1811. [\[CrossRef\]](#)
16. Giordano, G.; Klass, V.; Behm, M.; Lindbergh, G.; Sjöberg, J. Model-based lithium-ion battery resistance estimation from electric vehicle operating data. *IEEE Trans. Veh. Technol.* **2018**, *67*, 3720–3728. [\[CrossRef\]](#)
17. Hannan, M.A.; Hoque, M.D.M.; Hussain, A.; Yusof, Y.; Ker, A.P.J. State-of-the-Art and Energy Management System of Lithium-Ion Batteries in Electric Vehicle Applications: Issues and Recommendations. *IEEE Access* **2018**, *6*, 19362–19378. [\[CrossRef\]](#)
18. Han, X.; Wang, Z.; Wei, Z. A novel approach for health management online-monitoring of lithium-ion batteries based on model-data fusion. *Appl. Energy* **2021**, *302*, 117511. [\[CrossRef\]](#)
19. Lahsini, M.; Ben Belgacem, Y.; Khaldi, C.; Lamoumi, J. Kinetics and corrosion properties of the LaY₂Ni₉ alloy used as anode for nickel-metal hydride batteries. In Proceedings of the 2018 9th International Renewable Energy Congress (IREC), Hammamet, Tunisia, 20–22 March 2018; pp. 1–5. [\[CrossRef\]](#)
20. Zayani, W.; Azizi, S.; El-Nasser, K.S.; Ali, I.O.; Mathlouthi, H. Structural and electrochemical characterization of new co-doped spinel ferrite nanomaterial used as negative electrode in Ni/MH battery. In Proceedings of the 2018 9th International Renewable Energy Congress (IREC), Hammamet, Tunisia, 20–22 March 2018; pp. 1–5. [\[CrossRef\]](#)
21. Ortiz, J.P.; Valladolid, J.D.; Garcia, C.L.; Novillo, G.; Berrezueta, F. Analysis of machine learning techniques for the intelligent diagnosis of Ni-MH battery cells. In Proceedings of the 2018 IEEE International Autumn Meeting on Power, Electronics and Computing (ROPEC), Ixtapa, Mexico, 14–16 November 2018; pp. 1–6. [\[CrossRef\]](#)
22. Soltani, M.; Ben Belgacem, Y.; Telmoudi, A.J.; Chaari, A. Parameter identification and state of health evaluation for Nickel- Metal Hydride batteries based on an improved clustering algorithm. In Proceedings of the 2018 5th International Conference on Control, Decision and Information Technologies (CoDIT), Thessaloniki, Greece, 10–13 April 2018; pp. 128–133. [\[CrossRef\]](#)
23. Madusanka, S.; Mahadiulwewa, D.; Samarakoon, S.; Sandeepanie, K.; Damayanthi, R. Improving the Performance of Lead Acid Batteries using Nano-Technology. In Proceedings of the 2019 Moratuwa Engineering Research Conference (MERCon), Moratuwa, Sri Lanka, 3–5 July 2019; pp. 589–593. [\[CrossRef\]](#)
24. Caruso, M.; Castiglia, V.; Miceli, R.; Nevoloso, C.; Romano, P.; Schettino, G.; Viola, F.; Insinga, M.; Moncada, A.; Oliveri, R.; et al. Nanostructured lead acid battery for electric vehicles applications. In Proceedings of the 2017 International Conference of Electrical and Electronic Technologies for Automotive, Turin, Italy, 15–16 June 2017. [\[CrossRef\]](#)
25. Rosewater, D.M.; Copp, D.A.; Nguyen, T.A.; Byrne, R.H.; Santoso, S. Battery Energy Storage Models for Optimal Control. *IEEE Access* **2019**, *7*, 178357–178391. [\[CrossRef\]](#)
26. Liu, X.L.; Cheng, Z.M.; Yi, F.Y.; Qiu, T.Y. SOC calculation method based on extended Kalman filter of power battery for electric vehicle. In Proceedings of the 2017 12th International Conference on Intelligent Systems and Knowledge Engineering (ISKE), Nanjing, China, 24–26 November 2017. [\[CrossRef\]](#)
27. Guo, L.; Hu, C.; Li, G. The SOC estimation of battery based on the method of improved Ampere-hour and Kalman filter. In Proceedings of the 2015 IEEE 10th Conference on Industrial Electronics and Applications (ICIEA), Auckland, New Zealand, 15–17 June 2015; pp. 1458–1460. [\[CrossRef\]](#)
28. Coleman, M.; Lee, C.K.; Zhu, C.; Hurley, W.G. State-of-charge determination from EMF voltage estimation: Using impedance, terminal voltage, and current for lead-acid and lithium-ion batteries. *IEEE Trans. Ind. Electron.* **2007**, *54*, 2550–2557. [\[CrossRef\]](#)
29. Montenegro, D.; Rodríguez, S.; Fúelagán, J.R.; Jiménez, J.B. An Estimation Method of State of Charge and Lifetime for Lead-Acid Batteries in Smart Grid. In Proceedings of the 2015 IEEE PES Innovative Smart Grid Technologies Latin America (ISGT LATAM), Montevideo, Uruguay, 5–7 October 2015; pp. 564–569.
30. Al Mahmud, A.; Jafar, I.B.; Zaman, A.; Rahman, M. Performance study of lead-acid battery in a solar car under different traffic and weather conditions. In Proceedings of the 2016 4th International Conference on the Development in the in Renewable Energy Technology (ICDRET), Dhaka, Bangladesh, 7–9 January 2016; pp. 21–24. [\[CrossRef\]](#)
31. Dos Santos, G.S.; Grandinetti, F.J.; Alves, R.A.R.; de Queiróz Lamas, W. Design and simulation of an energy storage system with batteries lead acid and lithium-ion for an electric vehicle: Battery vs. conduction cycle efficiency analysis. *IEEE Lat. Am. Trans.* **2020**, *18*, 1345–1352. [\[CrossRef\]](#)
32. Wang, W. The electrochemical characteristics of AB₄-type rare earth–Mg–Ni-based superlattice structure hydrogen storage alloys for nickel metal hydride battery. *J. Magnes. Alloy.* **2021**, *9*, 2039–2048. [\[CrossRef\]](#)